

Results on θ_{13} Neutrino Oscillations from Reactor Experiments

Soo-Bong Kim

KNRC, Department of Physics and Astronomy, Seoul National University, Seoul 151-742, Korea

Abstract. Definitive measurements of the smallest neutrino mixing angle θ_{13} were made by Daya Bay, Double Chooz and RENO in 2012, based on the disappearance of electron antineutrinos emitted from reactors. The new generation reactor experiments have significantly improved a sensitivity for θ_{13} down to the $\sin^2(2\theta_{13}) \sim 0.01$ level using two identical detectors of 10 ~ 40 tons at near (300 ~ 400 m) and far (1 ~ 2 km) locations. The θ_{13} measurements by the three reactor experiments are presented with their future expected sensitivities.

1 Measurement of the Last and Smallest Neutrino Mixing Angle

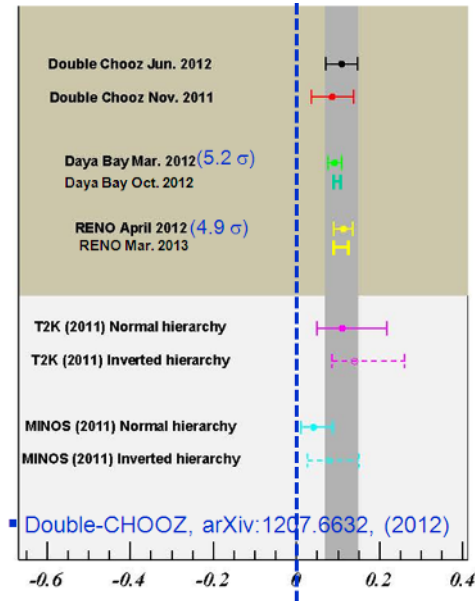
In the presently accepted paradigm to describe the neutrino oscillations, there are three mixing angles (θ_{12} , θ_{23} and θ_{13}) and one phase angle in the Pontecorvo-Maki-Nakagawa-Sakata matrix [1, 2]. Neutrino oscillation was discovered in the atmospheric neutrino by the Super-Kamiokande experiment in 1998 [3]. It was until 2012 that θ_{13} was the most poorly known as the smallest mixing angle. It took 14 years to measure all of the three mixing angles. Next round of neutrino experiments are expected to determine the neutrino mass hierarchy and the CP violation phase angle.

Measurements of θ_{13} are possible using reactor neutrinos and accelerator neutrino beams. Reactor measurements can determine the mixing angle without the ambiguities associated matter effects and CP violation. The reactor neutrino detector is not necessarily large, and construction of a neutrino beam is not needed. Past reactor experiments had a single detector located about 1 km from reactors. The new generation reactor experiments, Daya Bay, Double Chooz and RENO, have significantly reduced uncertainties associated with the measurement of θ_{13} using two identically performing detectors at near and far locations from reactors. An accurate value of θ_{13} by the reactor experiment will be able to offer the first glimpse of the CP phase angle, if combined with a result from an accelerator neutrino beam experiment.

Previous attempts of measuring θ_{13} have obtained only upper limits of $\sin^2(2\theta_{13}) < 0.15$ (90% C.L.) [4, 5]. Indications of a nonzero θ_{13} value were reported by two accelerator appearance experiments, T2K [6] and MINOS [7], and by the Double Chooz reactor disappearance experiment in 2011 [8]. Global analyses of all available neutrino oscillation data have indicated central values of $\sin^2(2\theta_{13})$ that are between 0.05 and 0.1 (see e.g., [9, 10]). In 2012, Daya Bay and RENO reported definitive measurements of the mixing angle θ_{13} based on the disappearance of reactor electron antineutrinos [11, 12]. A combined result of the θ_{13} measurements was reported by the Particle Data Group as $\sin^2(2\theta_{13}) = 0.098 \pm 0.013$ in ref. [13]. Measured values of θ_{13} by the second generation reactor experiments are summarized in Table 1 and Fig. 1.

Table 1. Summary of θ_{13} measurements by three reactor experiments.

| Experiments | Measured Value of $\sin^2(2\theta_{13})$ | Time |
|--------------|--|---------------|
| Double Chooz | 0.085 ± 0.051 | November 2011 |
| Daya Bay | 0.092 ± 0.017 | March 2012 |
| RENO | 0.113 ± 0.023 | April 2012 |
| Double Chooz | 0.109 ± 0.039 | June 2012 |
| Daya Bay | 0.089 ± 0.011 | October 2012 |
| RENO | 0.100 ± 0.018 | March 2013 |

**Figure 1.** Summary of measured θ_{13} values. This figure is taken from Ref. [18], and is updated with additional, recent measurements of Daya Bay and RENO which are described in Chapter 3.

2 Overview of Current Reactor Neutrino Experiments

2.1 Principle of θ_{13} measurement

Reactor experiments with a baseline distance of ~ 1 km can neglect the disappearance of electron antineutrinos driven by θ_{12} and Δm_{21}^2 and, thus, unambiguously determine the mixing angle θ_{13} based on the survival probability of electron antineutrinos,

$$P_{\text{survival}} \approx 1 - \sin^2 2\theta_{13} \sin^2(1.267\Delta m_{31}^2 L/E) \quad (1)$$

where E is the energy of antineutrinos in MeV, and L is the baseline distance in meters between the reactor and detector. The well measured value of $\Delta m_{32}^2 = (2.32^{+0.12}_{-0.08}) \times 10^{-3} \text{ eV}^2$ [13] can be substituted for Δm_{31}^2 in Eq. (1).

Two identical antineutrino detectors are located at near and far locations from reactors to allow a relative measurement from a comparison of the measured neutrino rates. The measured far-to-near

ratio of antineutrino fluxes can considerably reduce systematic errors coming from uncertainties in the reactor neutrino flux, target mass, and detection efficiency.

2.2 Detection method and detector for reactor antineutrinos

A nuclear reactor produces about 10^{20} antineutrinos per GW and per second, mainly coming from the beta decays of fission products of ^{235}U , ^{238}U , ^{239}Pu , and ^{241}Pu . The reactor antineutrino is detected via the inverse beta decay (IBD) reaction, electron antineutrino + proton \rightarrow positron + neutron. Reactor neutrino detectors based on hydrocarbon liquid scintillator (LS) provide free protons as a target. The coincidence of a prompt positron signal and a delayed signal from neutron capture by Gadolinium (Gd) provides the distinctive IBD signature.

The three reactor experiments have similar detector designs. A detector consists of a main inner part (ID) and an outer veto part (OD). The main detector is contained in a cylindrical stainless steel vessel that houses two nested cylindrical acrylic vessels. The inner most acrylic vessel holds $\sim 0.1\%$ Gd-doped LS as a neutrino target. It is surrounded by a gamma-catcher region with Gd-unloaded LS inside an outer acrylic vessel. Outside the gamma catcher is a buffer region with mineral oil. Light signals emitted from particles interacting in the main detector are detected by photomultiplier tubes that are mounted on the inner wall of the stainless steel container.

2.3 Description of three reactor experiments

The RENO experiment has a near detector and a far detector at the Hanbit (Yonggwang) nuclear power plant consisting of six well-aligned and equal-distant reactors, in South Korea. The Daya Bay experiment has two near detectors at two different locations and a far detector, at the Daya Bay nuclear power plant consisting of six reactors, in the southern part of China. The Double Chooz experiment has a far detector only at present and a near detector currently under construction at the Chooz nuclear power plant consisting of two reactors, in France.

Three reactor experiments have similar experimental arrangements, but slightly different features in reactor thermal output, detector target mass and overburden, and baselines of near and far detectors. Comparison of their interesting parameters is given in Table 2.

Table 2. Comparison of three reactor experimental parameters.

| Experiments | Location | Thermal Power (GW) | Flux Weighted Baselines Near/Far (m) | Overburden Near/Far (mwe) | Target Mass (tons) | Event Yield per Year (GW-ton-year) |
|--------------|----------|--------------------|--------------------------------------|---------------------------|--------------------|------------------------------------|
| Double Chooz | France | 8.5 | 410/1050* | 120/300 | 8.6/8.6 | 73 |
| RENO | Korea | 16.8 | 409/1444 | 120/450 | 16/16 | 267 |
| Daya Bay | China | 17.4 | 470 & 576/1648 | 250/860 | 40+40/80 | 1392 |

(* Geographical baselines without neutrino flux weighting)

3 Experimental Status

The first generation reactor experiments of Chooz and Paolo Verde could not continue data-taking longer than a half year because of unexpected problems with Gd-doped LS [4, 5]. Paolo Verde had problems with precipitation, condensation, and slow deterioration of Gd-doped LS developing in time. In Chooz experiment, Gd-doped LS turned yellow a few months after deployment. A rapid decay of attenuation length of Gd-doped LS had been observed. It is crucial for a reactor experiment to keep LS chemically stable for several years of experimental duration. The second generation reactor experiments were successful to develop Gd compounds, and have not suffered yet from the troubles that Chooz and Paolo Verde experienced.

RENO was the first reactor experiment to take data with both near and far detectors in operation from August 2011. The RENO collaboration reported a definitive measurement of θ_{13} based on 220 days of data taken through March 2012 as $\sin^2(2\theta_{13}) = 0.113 \pm 0.013(\text{stat.}) \pm 0.019(\text{syst.})$ in April 2012 [12]. An improved result of $\sin^2(2\theta_{13}) = 0.100 \pm 0.010(\text{stat.}) \pm 0.015(\text{syst.})$ was reported based on ~400 days of data through October 2012 at 2013 Neutrino Telescope workshop held in Venice, Italy [14]. The improvements came from better understanding of the detector energy scale, more accurate estimation of a cosmic ray induced background uncertainty, and more data. The RENO collaboration has been performing an analysis of energy-dependent neutrino oscillation effects and an effort of reducing the background uncertainty. They are expected to obtain a more precise measurement of the θ_{13} value from about 700 days of data set in the fall of 2013.

Daya Bay began data-taking with a part of near detectors from August 2012, and with 75% near and far detectors in operation from late December 2011. The Daya Bay collaboration reported a measured value of θ_{13} as $\sin^2(2\theta_{13}) = 0.092 \pm 0.016(\text{stat.}) \pm 0.005(\text{syst.})$ in March 2012 [11]. Data-taking was temporarily stopped in August 2012 to complete the rest of detector construction, and resumed in October 2012. An updated result of $\sin^2(2\theta_{13}) = 0.089 \pm 0.010(\text{stat.}) \pm 0.005(\text{syst.})$ was reported based on 140 days of data through May 2012 [15]. The collaboration is expected to have a doubled statistics of data set through July 2013, and obtain a new result on θ_{13} from both rate and shape analysis.

Double Chooz has been taking data with a far detector only since April 2011, and reported an evidence non-zero value of θ_{13} as $\sin^2(2\theta_{13}) = 0.085 \pm 0.029(\text{stat.}) \pm 0.042(\text{syst.})$ in November 2011 [16], and as $\sin^2(2\theta_{13}) = 0.086 \pm 0.041(\text{stat.}) \pm 0.030(\text{syst.})$ in March 2012 [17]. An updated result of $\sin^2(2\theta_{13}) = 0.109 \pm 0.030(\text{stat.}) \pm 0.025(\text{syst.})$ was reported based on an improved analysis on rate and energy shape with 228 days of data [18]. The collaboration recently reported a θ_{13} measurement by identifying a delayed signal of neutron capture on Hydrogen: $\sin^2(2\theta_{13}) = 0.097 \pm 0.034(\text{stat.}) \pm 0.034(\text{syst.})$ [19]. A near detector is under construction, and will be ready for data-taking in spring 2014.

4 Results on Neutrino Mixing Angle θ_{13}

The three reactor experiments employ similar detector calibration, backgrounds, and data analysis like similar detector designs. Thus we present how to obtain a reactor neutrino event sample and measure the value of θ_{13} in case of the RENO experiment as an example.

4.1 Event trigger and energy calibration

Event triggers are formed by the number of PMTs with signals above a ~0.3 photoelectrons (p.e.) threshold (NHIT). An event is triggered and recorded for an IBD candidate if the main inner detector NHIT is larger than 90, corresponding to 0.5-0.6 MeV and well below the 1.02 MeV minimum energy of an IBD positron signal.

Energy calibration was made using radioactive sources and cosmic ray induced background event samples. Radioisotopes of ^{137}Cs , ^{68}Ge , ^{60}Co , and ^{252}Cf are periodically deployed in the target and gamma catcher by a step motorized pulley system in a glove box. Event energy is determined from the total p.e. charge (Q_{tot}) that is collected by the PMTs, corrected for light collection and response variation. The energy is assigned based on roughly 1 MeV per 250 p.e. that is determined from the peak energies of various radioactive sources deployed at the center of the detector target.

4.2 Reactor electron antineutrino sample

An IBD event requires a delayed signal from a neutron capture on Gd and, thus, the fiducial volume naturally becomes the entire target vessel region without any vertex position cuts. There is some spill-in of IBD events that occur outside the target and produce a neutron capture on Gd in the target, which enhances the detection efficiency.

The following criteria are applied to select IBD candidate events: (i) $Q_{\max}/Q_{\text{tot}} < 0.03$ and relatively large average p.e. charge in the PMTs adjacent to the maximum charged PMT with respect to Q_{\max} where Q_{\max} is the the maximum charge of a PMT, to eliminate PMT flasher events and external gamma ray events; (ii) a cut rejecting events that occur within a 1 ms window following a cosmic muon traversing the ID with a visible energy (E_{μ}) that is larger than 70 MeV, or with between 20 MeV and 70 MeV for OD NHIT > 50; (iii) events are rejected if they are within a 10 ms window following a cosmic muon traversing the ID if E_{μ} is larger than 1.5 GeV; (iv) $0.7 \text{ MeV} < E_p < 12.0 \text{ MeV}$; (v) $6 \text{ MeV} < E_d < 12.0 \text{ MeV}$ where E_p (E_d) is the energy of the prompt (delayed) event; (vi) $2 < \Delta t_{e+n} < 100 \mu\text{s}$ where Δt_{e+n} is the time difference between the prompt and delayed signals; (vii) a multiplicity requirement rejecting correlated coincidence pairs if they are accompanied by any preceding ID or OD trigger within a 100 μs window before their prompt candidate. The overall IBD detection efficiency is estimated to be $(73.4 \pm 1.2)\%$ using a Monte Carlo simulation (MC) and data.

The energy distribution of the delayed events in the final candidate sample peaks at 8 MeV, consistent with the average energy of gamma-rays from the neutron capture by Gd, as shown in Fig. 2. The neutron capture time is measured as $\sim 26 \text{ ms}$ as expected from the Gd concentration of 0.11% in LS, as shown in Fig. 3. They demonstrate identical performance of near and far detectors in the RENO experiment.

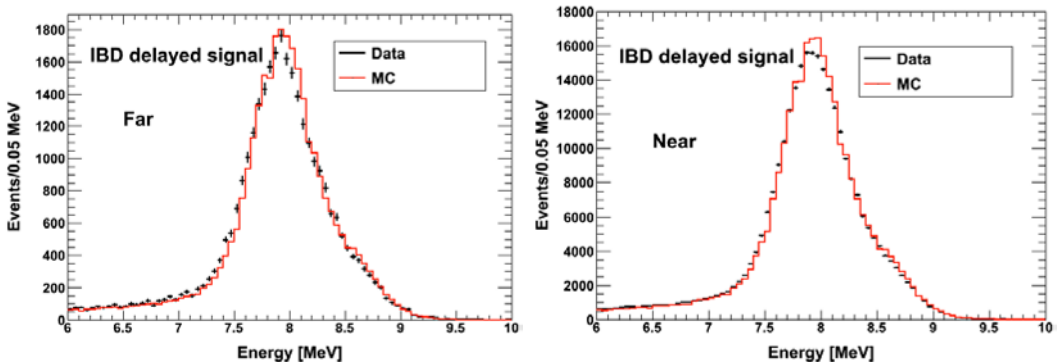


Figure 2. Energy distribution of the IBD delayed events in the final candidate sample.

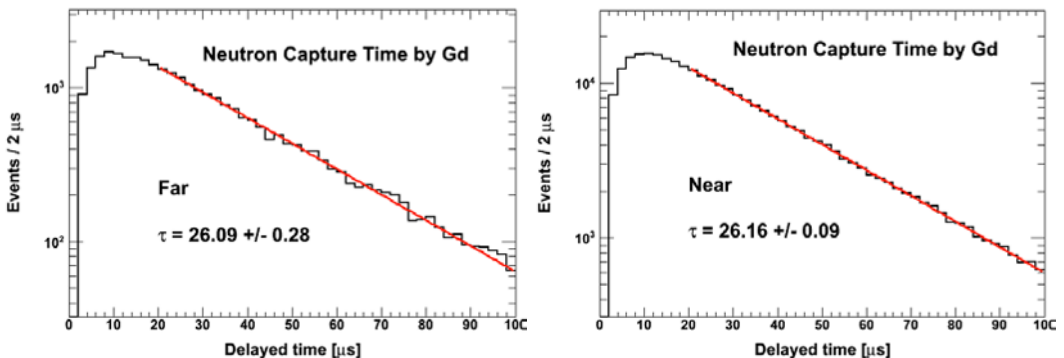


Figure 3. Neutron capture time distribution of the IBD delayed events in the final candidate sample.

4.3 Backgrounds

There are three remaining backgrounds in the final IBD candidate sample: (1) uncorrelated background of accidental coincidence from random association of prompt- and delayed-like events due to external gamma rays from radioactivity in the surrounding rock and detector noise events (accidentals), (2) correlated background due to energetic neutrons that are produced by cosmic muons traversing the surrounding rock and the detector, enter the ID, and interact in the target to produce a recoil proton as a prompt-like signal (fast neutrons), and (3) correlated background due to unstable isotopes of ${}^9\text{Li}/{}^8\text{He}$ that are produced by cosmic muons and decay into a positron and a neutron (${}^9\text{Li}/{}^8\text{He}$ β -n emitters).

In the final IBD candidate sample, the remained background is estimated to be 6.5% (2.7%) of the total far (near) events. The background shapes are also obtained from the background estimation. Fig. 4 shows the observed energy spectra of the IBD prompt events for the near and far detectors, exhibiting the reactor antineutrino spectra.

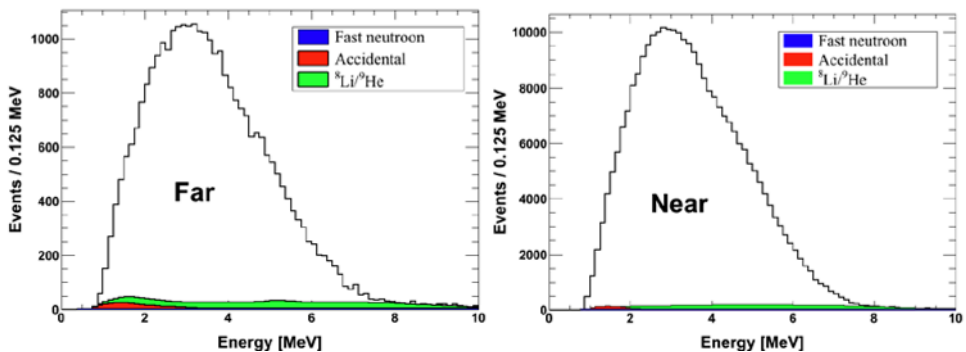


Figure 4. Observed energy spectra of the IBD prompt events with remaining backgrounds.

4.4 Observation of disappearance of reactor antineutrino

The reactor antineutrino flux depends on thermal power, fission fraction of the four main isotopes, energy released per fission, fission spectra, and fission and capture cross sections. The measured daily rates of IBD signals are compared with the expected rates assuming no oscillation that are obtained from the weighted fluxes by the thermal power and the fission fractions of each reactor and its baseline to each detector. The comparison of the far daily rates shows a clear deficit of the measured reactor neutrino flux.

The observed spectrum of IBD prompt signals in the far detector is compared to non-oscillation expectations based on measurements in the near detector in Fig. 5. The ratio of measured to expected events in the far detector indicates a clear deficit ($\sim 7\%$) of reactor electron antineutrinos. A deficit ($\sim 1\%$) of measured reactor neutrino flux is also observed to conclude that the observed reactor antineutrino disappearance is consistent with neutrino oscillations. The disappearance as a function of energy is also consistent with neutrino oscillations as shown in Fig. 5, and is under study to be used for a direct measurement of Δm_{31}^2 .

4.5 Measurement of neutrino mixing angle θ_{13}

The relative antineutrino-flux measurement of far-to-near ratio is independent of correlated uncertainties and helps minimize uncorrelated reactor uncertainties. The absolute uncertainties of the detection efficiency are correlated between the near and far detectors. The total uncorrelated uncertainty of detection efficiency is estimated to be 0.2% by taking differences between the two identical detectors. The uncorrelated uncertainty associated with reactor antineutrino flux is estimated

to be 0.9%, 0.5% due to the thermal output uncertainty and 0.7% due to the fission fraction uncertainty.

To determine the value of $\sin^2(2\theta_{13})$ from the deficit of the observed reactor neutrino flux, a χ^2 fit with pull terms on the uncorrelated systematic uncertainties was used to find $\sin^2(2\theta_{13}) = 0.100 \pm 0.010(\text{stat.}) \pm 0.015(\text{syst.})$ based on ~ 400 days of data through October 2012. The largest contribution to the systematic error is the uncertainty of the ${}^9\text{Li}/{}^8\text{He}$ background that will be significantly reduced by a new, better estimation method soon.

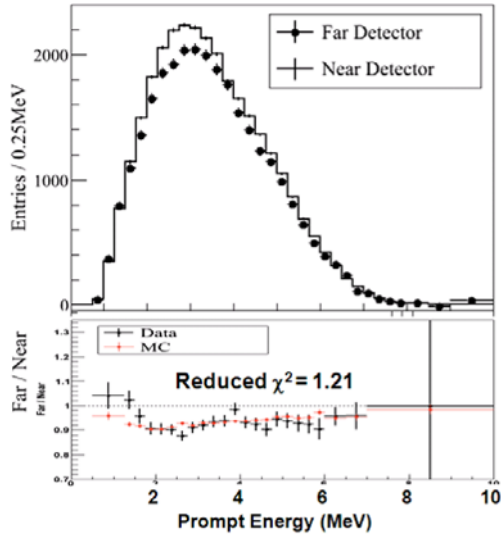


Figure 5. Observed spectra of the IBD prompt signal events in the far detector compared with the non-oscillation predictions from the measurements in the near detector.

Data-taking has been in a steady mode, and no detector degradation effect is seen yet. More data and reduction of systematic uncertainties will reduce the error of measured θ_{13} value. An analysis of energy-dependent neutrino oscillation is expected to provide more accurate measurement of the mixing angle.

5 Summary and Prospects

Three reactor experiments have definitively measured the value of θ_{13} by the disappearance of electron antineutrinos. Based on unprecedentedly copious data, Daya Bay and RENO have performed rather precise measurements of the value. Averaging the results of the three reactor experiments with the standard Particle Data Group method, one obtains $\sin^2(2\theta_{13}) = 0.098 \pm 0.013$ [13].

The exciting result provides a comprehensive picture of neutrino transformation among three kinds of neutrinos and opens the possibility of search for CP violation in the leptonic sector. The surprisingly large value of θ_{13} will strongly promote the next round of neutrino experiments to find CP violation effects and determine the neutrino mass hierarchy. The successful measurement of θ_{13} has made the very first step on the long journey to the complete understanding of the fundamental nature and implications of neutrino masses and mixing parameters.

Precise measurements of θ_{13} by the reactor experiments will provide the first glimpse of the CP phase angle if accelerator beam results are combined. Based on total 5 years of data, the reactor experiment is expected to obtain a measured $\sin^2(2\theta_{13})$ value with a precision of 7% at RENO, 4% at Daya Bay, and 10% at Double Chooz. It will also make a direct measurement of Δm_{31}^2 from the energy dependent oscillation effects, and measure a precise neutrino spectrum.

References

1. B. Pontecorvo, Sov. Phys. JETP **7**, 172 (1958)
2. Z. Maki, M. Nakagawa, and S. Sakata, Prog. Theor. Phys. **28**, 870 (1962)
3. Y. Fukuda *et al.*, Phys. Rev. Lett. **81**, 1562-1567 (1998)
4. M. Apollonio *et al.*, Phys. Lett. B **466**, 415 (1999); Eur. Phys. J. C **27**, 331 (2003)
5. F. Boehm *et al.*, Phys. Rev. Lett. **84**, 3764 (2000) ; Phys. Rev. D **64**, 112002 (2010)
6. K. Abe *et al.*, Phys. Rev. Lett. **107**, 041801 (2011)
7. P. Adamson *et al.*, Phys. Rev. Lett. **107**, 181802 (2011)
8. Y. Abe *et al.*, Phys. Rev. Lett. **108**, 131801 (2012)
9. G.L. Fogli *et al.*, Phys. Rev. D **84**, 053007 (2011)
10. T. Schwetz *et al.*, New J. Phys. **13**, 109401 (2011)
11. F.P. An *et al.*, Phys. Rev. Lett. **108**, 171803 (2012)
12. J.K. Ahn *et al.*, Phys. Rev. Lett. **108**, 191802 (2012)
13. J. Beringer *et al.* (Particle Data Group), Phys. Rev. D **86**, 010001 (2012)
14. See a talk given by Seon-Hee Seo at 15th Workshop on Neutrino Telescopes, Venice, Italy, 11-15 March, 2013.
15. F.P. An *et al.*, Chinese Physics C **37**, 011001 (2013)
16. See a talk given by Herve de Kerret at 6th Workshop on Low Energy Neutrino Physics, Seoul, Korea, 9-12 November, 2011.
17. Y. Abe *et al.*, Phys. Rev. Lett. **108**, 131801 (2012)
18. Y. Abe *et al.*, Phys. Rev. D **86**, 052008 (2012) ; arXiv :1207.6632 (2012).
19. Y. Abe *et al.*, Phys. Lett. B **723**, 66-70 (2013)